Observational Study

Medicine®

OPEN

Myocardial perfusion at rest in uncomplicated type 2 diabetes patients without coronary artery disease evaluated by 320-multidetector computed tomography

A pilot study

Xiangyi Cai, MD[a], Shuihua Zhang, MD[a], Dabiao Deng, MD[b], Honglin Li, MD[a], Xueqing Guan, MD[a], Jin Fang, MD[a], Quan Zhou, MD, PhD[a,*]

Abstract

Using computed tomography myocardial perfusion imaging (CTP) to investigate resting myocardial perfusion alterations in uncomplicated type 2 diabetes mellitus (T2DM) patients without obstructive coronary artery disease (CAD).

A total of 34 participants with 544 myocardial segments were included prospectively: 17 uncomplicated T2DM patients with no significant coronary artery stenosis on coronary computed tomography angiography and 17 healthy controls. Myocardial perfusion was evaluated by transmural perfusion ratio (TPR). Parameters of cardiac structure and function were measured for cardiac comprehensive assessment. Analyses included descriptive statistics and group comparisons.

TPR of segments 5, 7, 9, 10 to 14 were significantly reduced in T2DM group compared with controls ($P < .05$). When 16 myocardial segments were localized into different areas according to the wall orientations, axial levels of left ventricle and coronary artery territories, respectively, TPR of each area in T2DM group were significantly lower than those in the control group ($P < .05$). No significant differences were found in cardiac anatomy and function analyses between 2 groups.

In uncomplicated T2DM patients without obstructive CAD, myocardial perfusion impairments were present and may develop prior to cardiac morphological and functional abnormalities, which can be early detected by CTP.

Abbreviations: BMI = body mass index, BSA = body surface area, CAD = coronary artery disease, CCTA = coronary computed tomography angiography, CO = cardiac output, CT = computed tomography, CTP = computed tomography myocardial perfusion imaging, EDV = end-diastolic volume, EF = ejection fraction, ESV = end-systolic volume, IST_{dia} = end-diastolic interventricular septal thickness, IST_{sys} = end-systolic interventricular septal thickness, LAD = left anterior descending, LCX = left circumflex coronary artery, LV = left ventricular, $LVID_{dia}$ = end-diastolic left ventricular internal diameter, $LVID_{sys}$ = end-systolic left ventricular internal diameter, LVMI = left ventricular mass index, LVMM = left ventricular myocardial mass, MDCT = multidetector computed tomography, PWT_{dia} = end-diastolic posterior wall thickness, PWT_{sys} = end-systolic posterior wall thickness, RCA = right coronary artery, SPECT = single-photon emission computed tomography, SV = stroke volume, T2DM = type 2 diabetes mellitus, TPR = transmural perfusion ratio.

Keywords: computed tomography, diabetes mellitus, myocardial perfusion imaging, transmural perfusion ratio

1. Introduction

Cardiovascular disease remains the leading cause of mortality among type 2 diabetes mellitus (T2DM) patients, and approximately 40% of deaths are attributable to ischemic heart disease.[1] Silent myocardial ischemia is common in diabetes, even in the absence of coronary artery disease (CAD).[2,3] Therefore, early identification of myocardial ischemia shows great importance to diabetic people, which can help to make targeted intervention strategy and reduce mortality in this population.

In asymptomatic diabetic patients, stress-induced myocardial ischemia has been widely identified by radionuclide imaging.[4–6] Nevertheless, the issue of myocardial perfusion changes at rest in these patients remains disputable. Djaberi et al[4] proved that abnormal myocardial perfusion in diabetic patients without obstructive epicardial CAD was associated with endothelial dysfunction, and also proposed myocardial hypoperfusion may occur during rest. However, a single-photon emission computed tomography (SPECT) research demonstrated normal resting myocardial perfusion in T2DM patients without CAD.[6] Thus,

Editor: Liang-Jun Yan.

Xiangyi Cai and Shuihua Zhang have contributed equally to this study.

This study was supported by the National Natural Science Foundation of China (Grant Numbers 81471659 and 81630046).

The authors have no conflicts of interest to disclose.

[a] *Medical Imaging Center, First Affiliated Hospital of Jinan University,* [b] *Department of Radiology, Guangdong 999 Brain Hospital, Guangzhou, Guangdong, China.*

[*] *Correspondence: Quan Zhou, Department of Radiology, Medical Imaging Center, The First Affiliated Hospital, Jinan University, No. 613 West Huangpu Avenue, Tianhe, Guangzhou, Guangdong 510630, China (e-mail: oimaging@jnu.edu.cn).*

Medicine (2018) 97:5(e9762)

Received: 19 June 2017 / Received in final form: 12 December 2017 / Accepted: 11 January 2018

http://dx.doi.org/10.1097/MD.0000000000009762

whether resting myocardial perfusion abnormalities can be observed in diabetic patients without CAD is still uncertain.

The improvements of multidetector computed tomography (MDCT) have made it possible to simultaneously evaluate coronary anatomy, cardiac function, and myocardial perfusion in a 1-shot scan, with the combination of coronary computed tomography angiography (CCTA) and computed tomography myocardial perfusion imaging (CTP).[7–10] In particular, the myocardial transmural perfusion ratio (TPR) calculated from CTP provides quantitative information of myocardial hemodynamics.[7]

The objective of our study was using 320-MDCT to investigate myocardial perfusion at rest in uncomplicated T2DM patients without obstructive CAD. Besides, we also aim to assess parameters of left ventricular (LV) structures and cardiac function to make a comprehensive analysis.

2. Materials and methods

2.1. Study population

In this prospective study, asymptomatic T2DM patients who were screened for cardiovascular diseases were enrolled consecutively. The diagnosis of T2DM was made according to the guidelines of the American Diabetes Association's Standards.[11] Individuals were excluded with any of the following characteristics: with significant coronary abnormalities on CCTA, including coronary artery calcium, obstructive CAD which is defined as visible coronary plaque and luminal stenosis on CCTA according to SCCT guidelines,[12] coronary stent implantation and coronary bypass; hypertension, serious cardiac arrhythmia, congenital heart disease, primary cardiomyopathy, and other known cardiovascular diseases; diabetes associated complications (nephropathy, retinopathy, neuropathy, etc.); and intolerance to iodinated contrast medium, pregnancy or other contraindications to performing cardiac computed tomography (CT).

From August 2015 to January 2017, 68 T2DM patients were enrolled in the study; 51 patients (75%) were excluded due to hypertension, serious cardiac arrhythmia, and other cardiovascular diseases. Significant coronary abnormalities on CCTA were identified in 35 patients (51%), pool imaging quality caused by motion artifacts was present in 2 patients, and thus these patients were excluded. The remaining 17 patients were included and constituted the T2DM group. Seventeen gender and age-matched nondiabetic healthy subjects were recruited from the physical examination center and constituted the control group.

The study was approved by our institutional review board, and all patients voluntarily signed the informed consent.

2.2. Cardiac CT protocol

All the participants underwent CCTA/rest CTP examinations by a 320-detector dynamic volumetric CT (Aquilion One, Toshiba Medical Systems, Otawara, Japan). The scanner was implemented with following parameters: collimation, 320×0.5 mm (320-detector rows $\times$ 0.5-mm-thick sections); velocity of gantry rotation, 0.35 s/r; pitch, 0.2 to 0.3; tube voltage was set according to the body mass index (BMI) of the participant (100 kV for BMI < 23, 120 kV for BMI ≥ 23); automatic tube current. A volume of 40 to 60 mL nonionic contrast medium (Iopromide Injection [370 mg iodine per milliliter], Bayer Pharma AG, Berlin, Germany) was used at injection rate of 4.0 to 6.0 mL/s. The scan was triggered by Sure Start software, configured descending aorta as region of interest with a threshold of 240 HU. With retrospective electrocardiogram-gated algorithm, the exposure scope was obtained automatically depending on heart rate, and scanned for 1 to 2 cardiac cycle.

2.3. Images processing and analysis

The images of cardiac CT were evaluated by 2 qualified observers who were unaware of the clinical information independently. All the images of myocardial perfusion, LV structures, and cardiac function were processed and analyzed on the postprocessing workstation (Vitrea FX, Vital Images, Minnetonka, MN). Myocardial perfusion at rest was evaluated by TPR (Fig. 1), which was defined as the ratio of subendocardial attenuation density to subepicardial attenuation density.[7] The subendocardial and subepicardial contours of LV myocardium were automatically detected and manually corrected to avoid inclusion of blood pool or extraventricular tissue. TPR in each myocardial segment was identified using standardized 17 segments model of the American Heart Association statement (except S17/the apex).[13] Besides, myocardial segments were localized with the reference to wall orientations on short-axis views: anterior wall (segments 1, 7, and 13), inferior wall (segments 4, 10, and 15), septal wall (segments 2, 3, 8, 9, and 14), and lateral wall (segments 5, 6, 11, 12, and 16). According to the levels on long-axis of left ventricle, basal was defined as segments 1 to 6, mid as segments 7 to 12 and apical as segments 13 to 16. Myocardium were also divided by coronary artery territories: left anterior descending artery (LAD) territories (segments 1, 2, 7, 8, 13, 14, and 17), left circumflex coronary artery (LCX) territories (segments 5, 6, 11, 12, and 16), and right coronary artery (RCA) territories (segments 3, 4, 9, 10, and 15).[13]

Cardiac imaging datasets were reconstructed for 10 phases with 10% of the interval and loaded into the cardiac function analysis software. The structural parameters were manually measured on multiplanar reformations according to the guidelines for cardiac chamber quantification.[14] The structural parameters included end-systolic left ventricular internal diameter ($LVID_{sys}$), end-systolic posterior wall thickness (PWT_{sys}), end-systolic interventricular septal thickness (IST_{sys}), end-diastolic left ventricular internal diameter ($LVID_{dia}$), end-diastolic posterior wall thickness (PWT_{dia}), and end-diastolic interventricular septal thickness (IST_{dia}), which were obtained by manual measuring.[15,16] Measurements in end-systole and end-diastole were identified at the same orientation and level. The subendocardial and subepicardial borders of LV myocardium were automatically described and manually corrected.[16] The functional parameters including ejection fraction (EF), end-systolic volume (ESV), end-diastolic volume (EDV), stroke volume (SV), cardiac output (CO), left ventricular myocardial mass (LVMM), as well as body surface area (BSA) were automatically calculated according to height and weight. Left ventricular mass index (LVMI) was defined as LVMM divided by BSA.[15]

2.4. Statistical analysis

Statistical analysis was performed by SPSS 21.0 software. Continuous variables were expressed as mean $\pm$ standard deviation and categorical variables as numbers and percentages. To compare the baseline characteristics, TPR, structural, and cardiac function parameters between 2 groups, the Student t test and Mann–Whitney U test were used. A P value of $<.05$ was considered statistically significant. Interobserver variability was

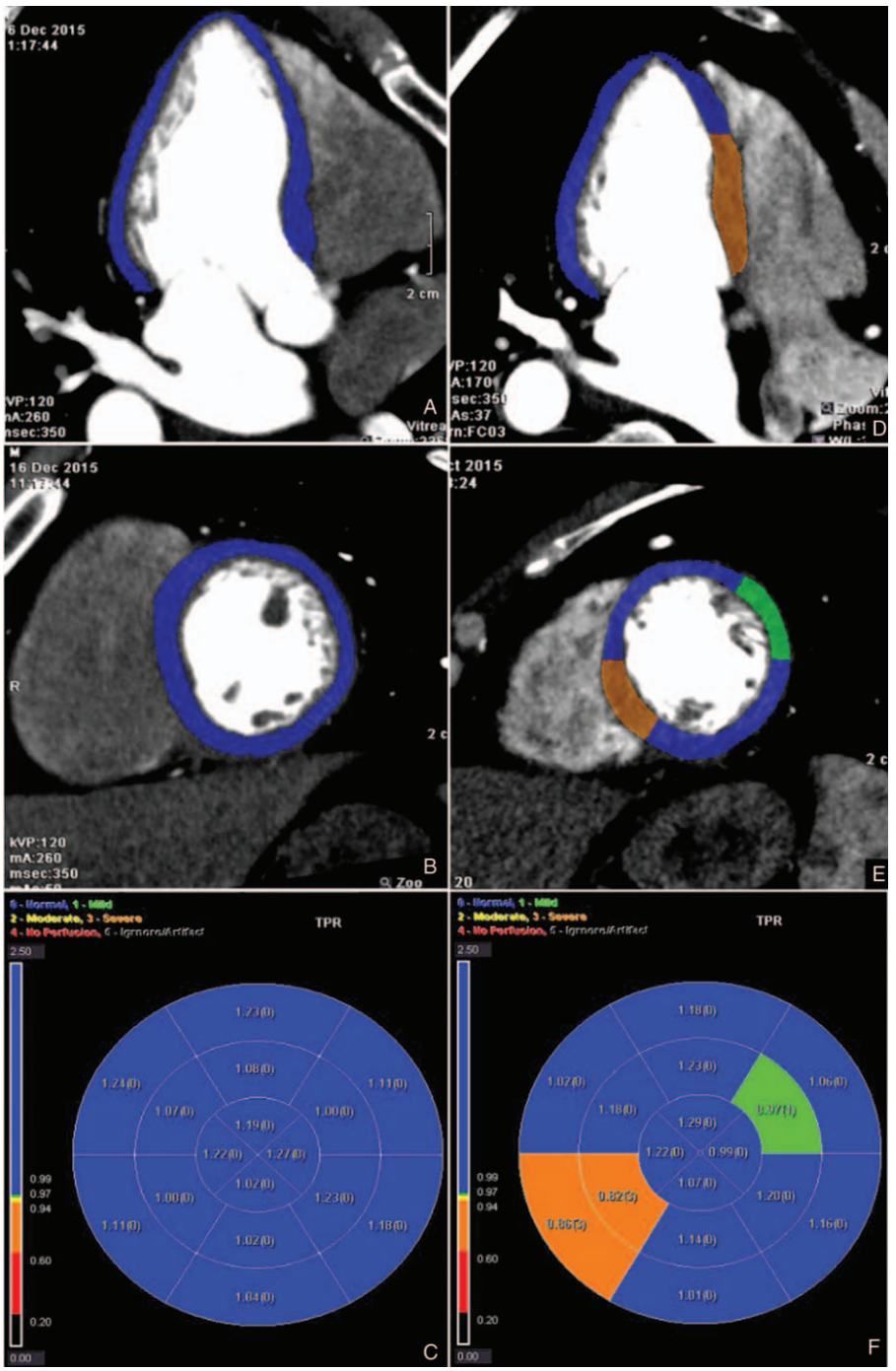

Figure 1. Rest computed tomography perfusion images in 4-champer projection, short-axis projection, and polar maps of transmural perfusion ratio (TPR). Normal rest myocardial perfusion images from a healthy participant as in A–C. TPR in 16 segments of the left ventricular myocardium shows blue color, which indicates normal myocardial perfusion (TPR values > 0.99). Abnormal rest myocardial perfusion images from a type 2 diabetes patient as in D–F. The TRP polar map shows green color in S12, which indicates mild perfusion abnormality ($0.97 <$ TPR values ≤ 0.99), orange color in S3 and S9 indicates severe perfusion abnormality ($0.60 <$ TPR values ≤ 0.9).

evaluated with Bland–Altman plot by using Med Calc 17.2 statistical software.

3. Results

3.1. Baseline characteristics

A total of 34 participants (aged 30–72 years) with 544 myocardial segments were included for analysis, consisted of 17 uncomplicated T2DM patients and 17 healthy controls. The baseline demographic and clinical characteristics of 2 groups were presented in Table 1. No significant differences were found in demographic characteristics between 2 groups, with the exception of fasting plasma glucose and HbA1c levels which was significantly higher in T2DM group ($P < .001$).

3.2. Radiation exposure

The effective radiation dose was calculated by the conversion coefficient K and dose–length–product according to the standard

Table 1

Clinical characteristics of the groups.

	Control group	T2DM group	*P*
Age, mean years (SD)	51 (2)	56 (2)	.09
Female, n (%)	10 (59)	8 (41)	1.00
T2DM duration, median years (IQR)	—	4 (2–10)	—
BMI, mean kg/m^2 (SD)	24 (1)	24 (1)	.60
Systolic BP, mean mm Hg (SD)	111 (3)	120 (3)	.10
Diastolic BP, mean mm Hg (SD)	68 (2)	73 (1)	.17
FPG, mean mmol/L (SD)	5.5 (0.1)	9.7 (1.1)	<.001
HbA1c, mean % (SD)	5.4 (0.1)	8.8 (0.7)	<.001
Total cholesterol, mean mmol/L (SD)	5.4 (0.2)	5.3 (0.3)	.68
Triglycerides, mean mmol/L (SD)	1.3 (0.2)	1.9 (0.5)	.29
HDL, mean mmol/L (SD)	1.3 (0.6)	1.2 (0.7)	.33
LDL, mean mmol/L (SD)	3.6 (0.2)	3.1 (0.3)	.13

BMI = body mass index, BP = blood pressure, FPG = fasting plasma glucose, HbA1c = glycated hemoglobin, HDL = high-density lipoprotein, IQR = interquartile range, LDL = low-density lipoprotein, SD = standard deviation, T2DM = type 2 diabetes mellitus.

Table 2

TPR of 16 segments in 2 groups.

	Control group	T2DM group	*P*
Overall			
Mean	1.14 ± 0.01	1.07 ± 0.01	<.001
Wall			
Anterior	1.15 ± 0.01	1.06 ± 0.02	.001
Inferior	1.14 ± 0.02	1.08 ± 0.02	.048
Septal	1.15 ± 0.02	1.08 ± 0.02	.001
Lateral	1.13 ± 0.01	1.06 ± 0.01	<.001
Axis			
Basal	1.14 ± 0.01	1.09 ± 0.01	.004
Mid	1.11 ± 0.01	1.02 ± 0.01	<.001
Apical	1.20 ± 0.02	1.12 ± 0.02	.003
Territories			
LAD	1.18 ± 0.01	1.10 ± 0.01	<.001
LCX	1.13 ± 0.01	1.06 ± 0.01	<.001
RCA	1.11 ± 0.01	1.05 ± 0.01	.001

Data presented as mean ± standard deviation.
LAD = left anterior descending, LCX = left circumflex coronary artery, RCA = right coronary artery, T2DM = type 2 diabetes mellitus, TPR = transmural perfusion ratio.

methodology outlined in the European Guidelines on Quality Criteria for Computed Tomography.[17] The effective radiation exposure for a CT scanning in the study was 5.53 ± 0.30 mSv.

3.3. CT myocardial perfusion, LV structures, and cardiac function

Bland–Altman plot for interobserver variability in TPR quantification is shown in Fig. 2. The mean difference was −0.02 with 95% limits of agreement from −0.22 to 0.18. Myocardial TPR in 2 groups is listed in Table 2. Distribution of TPR in 16 myocardial segments between 2 groups is shown in Fig. 3. The TPR of segments 5, 7, 9, 10 to 14 was significantly reduced in T2DM group ($P < .05$). TPR of other segments in T2DM group was also found to be decreased when compared with the control group, without reaching statistical significance. The mean TPR values of 16 segments for each individual were calculated, and patients in T2DM group were found to have a remarkably lower mean TPR than the controls ($P < .001$).

In addition, LV myocardium was further localized according to wall orientations (septal, anterior, lateral, inferior wall), axial levels of left ventricle (basal, mid, and apical) and coronary artery (LAD, LCX, and RCA) territories, respectively. Comparisons of TPR in the corresponding areas between 2 groups are listed in Table 2. The mean TPR of each localized area in the T2DM group was lower than those in the control group, and the lowest mean TPR (1.02) in the T2DM group was detected in the mid. TPR in different wall orientations (septal, anterior, lateral, and inferior wall) and axial levels of left ventricle (basal, mid, and apical) were significantly reduced in T2DM group ($P < .05$ and $P < .005$, respectively). For vessel-based analysis, TPR of LAD, LCX, and RCA supplied territories in T2DM group was also significantly lower than those in control group ($P < .005$).

Parameters of cardiac anatomy and function analyses in 2 groups are given in Table 3. In T2DM group, ESV, EDV, SV, CO, $LVID_{sys}$, and $LVID_{dia}$ were slightly decreased, whereas EF, LVMM, LVMI, PWT_{sys}, PWT_{dia}, IST_{sys}, and IST_{dia} were slightly increased compared with control group. However, no significant differences were found in cardiac anatomy and function analyses between 2 groups.

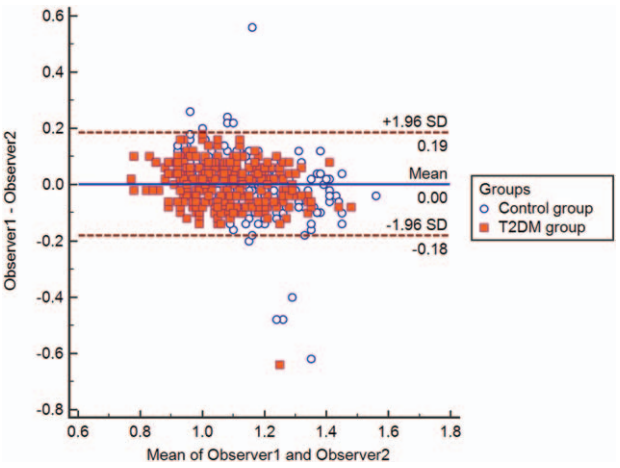

Figure 2. Bland–Altman plot for interobserver variability in transmural perfusion ratio quantification between observer 1 and observer 2.

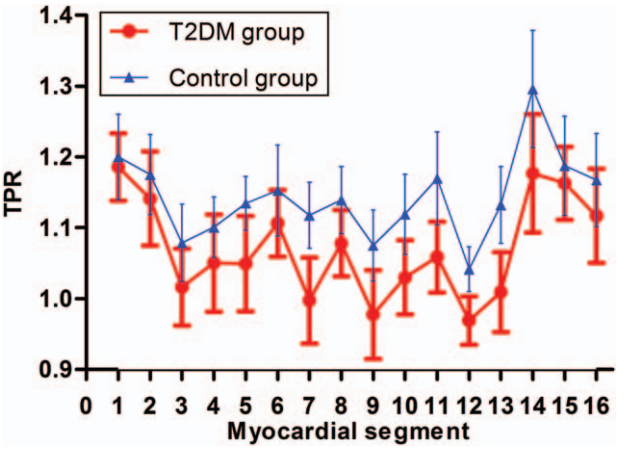

Figure 3. Distribution of transmural perfusion ratio (TPR) in 16 myocardial segments between 2 group (n = 544 myocardial segments). Error bars show 95% confidence intervals.

Table 3

Cardiac anatomy and function analyses.

	Control group	T2DM group	*P*
EF , %	65 ± 2	66 ± 2	1.00
ESV, mL	43 ± 4	37 ± 3	.24
EDV, mL	120 ± 5	108 ± 6	.15
SV, mL	77 ± 3	72 ± 4	.30
CO, L/min	4.7 ± 0.2	4.4 ± 0.2	.39
LVMM, g	75.4 ± 4.9	77.3 ± 4.1	.43
LVMI	43 ± 2	46 ± 2	.17
$LVID_{sys}$, mm	28.4 ± 0.9	28.3 ± 0.9	.97
PWT_{sys}, mm	13.0 ± 0.5	13.6 ± 0.8	.66
IST_{sys}, mm	11.9 ± 0.5	13.1 ± 0.6	.13
$LVID_{dia}$, mm	45.5 ± 1.1	44.7 ± 0.8	.53
PWT_{dia}, mm	7.4 ± 0.3	8.3 ± 0.4	.07
IST_{dia}, mm	8.1 ± 0.2	9.1 ± 0.4	.09

Data are presented as mean ± standard deviation.

CO = cardiac output, EDV = end-diastolic volume, EF = ejection fraction, ESV = end-systolic volume, IST_{dia} = end-diastolic interventricular septal thickness, IST_{sys} = end-systolic interventricular septal thickness, LAD_{sys} = end-systolic left atrial diameter, $LVID_{dia}$ = end-diastolic left ventricular internal diameter, $LVID_{sys}$ = end-systolic left ventricular internal diameter, LVMI = left ventricular mass index, LVMM = left ventricular myocardial mass, PWT_{dia} = end-diastolic posterior wall thickness, PWT_{sys} = end-systolic posterior wall thickness, SV = stroke volume, T2DM = type 2 diabetes mellitus.

4. Discussion

To the best of our knowledge, there are no previous studies using 320-MDCT to investigate myocardial perfusion at rest in uncomplicated T2DM patients without CAD. In this study, lower myocardial perfusion at rest was observed in T2DM group, whereas their LV structures and cardiac function parameters based on cardiac CT showed no difference compared with control group. The result of the present study suggests that in uncomplicated T2DM patients with no clinical evidences of obstructive CAD, myocardial perfusion impairment is present which may develop prior to cardiac morphological and functional abnormalities; and resting myocardial perfusion changes are detectable by 320-MDCT in pure T2DM patients without CAD, which would suggest a practical method to detect early preclinical myocardial impairment in diabetic heart.

Asymptomatic myocardial ischemia is frequent in diabetes, even in the absence of CAD.[2] An early study has shown a coronary flow reserve reduction in T2DM patients with normal coronary arteries.[18] Then myocardial perfusion defects were widely identified by radionuclide imaging in asymptomatic patients with diabetes, which were attributed to endothelial dysfunction and microvascular impairment.[4–6] In our study, myocardial TPR at rest of each segment or location in T2DM group was lower than those in healthy controls, which is similar to findings in previous studies. However, our finding is not consistent with a SPECT study that demonstrated normal myocardial perfusion at rest in T2DM patients without CAD.[6] This discrepancy could be partly due to different methods of testing and evaluating myocardial perfusion. Moreover, inclusion criteria of this SPECT research were comparatively restrictive, which may also contribute to the negative result of resting perfusion. Indeed, endothelial dysfunction has been shown to affect resting myocardial perfusion in early study.[19] Accordingly, reduction of microvascular perfusion at rest may be observed. Interestingly, we also noticed that the TPR of segment 5, 7, 9, 10 to 14 was significantly lower in T2DM patients. It suggests that these specific segments might be the vulnerable regions in diabetic heart, and further related studies are demanded to prove this conjecture.

The cardiac structure and function associated with diabetes are generally identified by ventricular dilatation and hypertrophy, diastolic and/or systolic dysfunction.[20,21] Diastolic dysfunction was common in asymptomatic T2DM patients, which may be the earliest change of diabetic heart.[22,23] In current study, however, parameters of cardiac anatomy and function were similar between uncomplicated T2DM patients and healthy controls. The negative result could be partly due to the exclusion of patients with hypertension, which is strongly associated with cardiac abnormalities in diabetes.[24] Another possible reason could be the diabetic duration was relatively short in patients of our study (median 4 years); therefore, long-term cardiac abnormalities were less likely to present among them.[25] Besides, the lack of significant difference in structural and function parameters between the 2 group may be related to the small study population, thus further confirmation is needed.

Importantly, lower myocardial perfusion at rest was observed in T2DM patients in absence of obstructive CAD, whereas LV structures and cardiac function measures based on cardiac CT were normal. These results suggest that the reduction of myocardial perfusion may be a significant early alteration of diabetes-induced myocardial impairment. Similar finding has been reported in a recent multicenter study that observed early perfusion abnormalities on dynamic CT in diabetes and hypertension patients.[26] However, this study included symptomatic patients with suspected or known CAD, and 66.7% of them presented coronary plaque or stenosis on CCTA. In contrast with the present study, we only included T2DM patients with normal coronary arteries, in order to find potential myocardial perfusion alterations in early stage of diabetes, independently of obstructive CAD. We now describe a similar effect in T2DM patients, and further found these changes occurred with normal cardiac and structures function.

It has been widely verified that CCTA can improve risk prediction for cardiac events and provide long-term prognostic information for T2DM patients.[27,28] In our study, CCTA and CT perfusion imaging were implemented in the meantime, which mean only a 1-shot scan can provide prognostic information as well as structural and functional assessment.[29] It is undisputed that the combination of CCTA and CTP fulfills a more comprehensive screening for the diabetes, which offers a new way for the early detection of cardiovascular complications. In particular, the wide-area detectors of 320-MDCT have an ability to image the entire heart simultaneously, with ultra-fast scan speed to reduce motion artifacts and lower radiation. Moreover, scan parameters were individualized to improve imaging quality, as well as reduce contrast dose and radiation exposure.[30]

5. Limitations

There are some limitations in the study. First, our result suggests that myocardial perfusion impairment develops prior to cardiac morphological and functional abnormalities in T2DM patients. But follow-up observation of the potential cardiac structure and function changes was not conducted in this study, and further cohort studies are demanded. Second, previous evidence demonstrated that impaired microvascular function caused by endothelial dysfunction occurred before the development of vascular structural changes or significant coronary artery stenosis,[2,21] which result in myocardial perfusion abnormalities in diabetic patients without CAD. However, we cannot provide direct evidence for these mechanisms, thus further studies are needed to examine. Third, radionuclide imaging was not implemented and

compared as the standard of myocardial perfusion imaging in our research. Indeed, previously researches have verified that CT perfusion imaging had good diagnostic accuracy and consistency for identifying myocardial ischemia compared with SPECT, when combined with CCTA.[7–9] Furthermore, we performed the CT perfusion imaging only in static state, for the concern of additional radiation exposure from the "2-step" rest–stress scan in comprehensive CT.[31] But subsequent studies have demonstrated that the rest TPR was similar to stress TPR in patients without coronary stenosis,[32] and thus sufficient diagnostic information can be derived from rest condition to some extent.[33] Lastly, this is a preliminary study based on a relatively small number of subjects in a single center; therefore, the conclusions need be further confirmed in a larger cohort follow-up research.

6. Conclusions

In conclusion, myocardial impairment can be detected in uncomplicated T2DM patients in the absence of obstructive CAD, even precedes cardiac structural and functional abnormalities. These changes are subtle; however, it provides additional information on myocardial impairment in diabetes, which might be useful to better identify the early stages of diabetic heart disease.

References

[1] Low Wang CC, Hess CN, Hiatt WR, et al. Clinical update: cardiovascular disease in diabetes mellitus: atherosclerotic cardiovascular disease and heart failure in type 2 diabetes mellitus—mechanisms, management, and clinical considerations. Circulation 2016;133:2459–502.

[2] Camici PG, Crea F. Medical progress—coronary microvascular dysfunction. N Engl J Med 2007;356:830–40.

[3] Di Carli MF, Janisse J, Grunberger G, et al. Role of chronic hyperglycemia in the pathogenesis of coronary microvascular dysfunction in diabetes. J Am Coll Cardiol 2003;41:1387–93.

[4] Djaberi R, Roodt JO, Schuijf JD, et al. Endothelial dysfunction in diabetic patients with abnormal myocardial perfusion in the absence of epicardial obstructive coronary artery disease. J Nucl Med 2009;50:1980–6.

[5] Roos CJ, Djaberi R, Schuijf JD, et al. Relationship between vascular stiffness and stress myocardial perfusion imaging in asymptomatic patients with diabetes. Eur J Nucl Med Mol Imaging 2011;38:2050–7.

[6] Marciano C, Galderisi M, Gargiulo P, et al. Effects of type 2 diabetes mellitus on coronary microvascular function and myocardial perfusion in patients without obstructive coronary artery disease. Eur J Nucl Med Mol Imaging 2012;39:1199–206.

[7] George RT, Arbab-Zadeh A, Miller JM, et al. Adenosine stress 64- and 256-row detector computed tomography angiography and perfusion imaging: a pilot study evaluating the transmural extent of perfusion abnormalities to predict atherosclerosis causing myocardial ischemia. Circ Cardiovasc Imaging 2009;2:174–82.

[8] Valdiviezo C, Ambrose M, Mehra V, et al. Quantitative and qualitative analysis and interpretation of CT perfusion imaging. J Nucl Cardiol 2010;17:1091–100.

[9] Cury RC, Magalhaes TA, Paladino AT, et al. Dipyridamole stress and rest transmural myocardial perfusion ratio evaluation by 64 detector-row computed tomography. J Cardiovasc Comput Tomogr 2011;5:443–8.

[10] Ko BS, Cameron JD, Leung M, et al. Combined CT coronary angiography and stress myocardial perfusion imaging for hemodynamically significant stenoses in patients with suspected coronary artery disease: a comparison with fractional flow reserve. JACC Cardiovasc Imaging 2012;5:1097–111.

[11] American Diabetes AssociationErratum. Classification and diagnosis of diabetes. Sec. 2. In Standards of Medical Care in Diabetes-2016. Diabetes Care 2016;39(Suppl. 1):S13–S22. Diabetes Care 2016;39:1653.

[12] Leipsic J, Abbara S, Achenbach S, et al. SCCT guidelines for the interpretation and reporting of coronary CT angiography: a report of the Society of Cardiovascular Computed Tomography Guidelines Committee. J Cardiovasc Comput Tomogr 2014;8:342–58.

[13] Cerqueira MD, Weissman NJ, Dilsizian V, et al. Standardized myocardial segmentation and nomenclature for tomographic imaging of the heart. A statement for healthcare professionals from the Cardiac Imaging Committee of the Council on Clinical Cardiology of the American Heart Association. Circulation 2002;105:539–42.

[14] Lang RM, Badano LP, Mor-Avi V, et al. Recommendations for cardiac chamber quantification by echocardiography in adults: an update from the American Society of Echocardiography and the European Association of Cardiovascular Imaging. Eur Heart J Cardiovasc Imaging 2015;16:233–70.

[15] Stolzmann P, Scheffel H, Leschka S, et al. Reference values for quantitative left ventricular and left atrial measurements in cardiac computed tomography. Eur Radiol 2008;18:1625–34.

[16] Kishi S, Magalhaes TA, George RT, et al. Relationship of left ventricular mass to coronary atherosclerosis and myocardial ischaemia: the CORE320 multicenter study. Eur Heart J Cardiovasc Imaging 2015;16:166–76.

[17] Shrimpton PC, Hillier MC, Lewis MA, et al. National survey of doses from CT in the UK: 2003. Br J Radiol 2006;79:968–80.

[18] Storto G, Pellegrino T, Sorrentino AR, et al. Estimation of coronary flow reserve by sestamibi imaging in type 2 diabetic patients with normal coronary arteries. J Nucl Cardiol 2007;14:194–9.

[19] Johnson NP, Gould KL. Clinical evaluation of a new concept: resting myocardial perfusion heterogeneity quantified by Markovian analysis of PET identifies coronary microvascular dysfunction and early atherosclerosis in 1,034 subjects. J Nucl Med 2005;46:1427–37.

[20] Pappachan JM, Varughese GI, Sriraman R, et al. Diabetic cardiomyopathy: pathophysiology, diagnostic evaluation and management. World J Diabetes 2013;4:177–89.

[21] Huynh K, Bernardo BC, McMullen JR, et al. Diabetic cardiomyopathy: mechanisms and new treatment strategies targeting antioxidant signaling pathways. Pharmacol Ther 2014;142:375–415.

[22] Brooks BA, Franjic B, Ban CR, et al. Diastolic dysfunction and abnormalities of the microcirculation in type 2 diabetes. Diabetes Obes Metab 2008;10:739–46.

[23] Vinereanu D, Nicolaides E, Tweddel AC, et al. Subclinical left ventricular dysfunction in asymptomatic patients with type II diabetes mellitus, related to serum lipids and glycated haemoglobin. Clin Sci (Lond) 2003;105:591–9.

[24] Scholte A, Schuijf J, Kharagjitsingh A, et al. Different manifestations of coronary artery disease by stress SPECT myocardial perfusion imaging, coronary calcium scoring, and multislice CT coronary angiography in asymptomatic patients with type 2 diabetes mellitus. J Nucl Cardiol 2008;15:503–9.

[25] Jorgensen PG, Jensen MT, Mogelvang R, et al. Impact of type 2 diabetes and duration of type 2 diabetes on cardiac structure and function. Int J Cardiol 2016;221:114–21.

[26] Vliegenthart R, De Cecco CN, Wichmann JL, et al. Dynamic CT myocardial perfusion imaging identifies early perfusion abnormalities in diabetes and hypertension: insights from a multicenter registry. J Cardiovasc Comput Tomogr 2016;10:301–8.

[27] Van Werkhoven JM, Cademartiri F, Seitun S, et al. Diabetes: prognostic value of CT coronary angiography—comparison with a nondiabetic population. Radiology 2010;256:83–92.

[28] Andreini D, Pontone G, Mushtaq S, et al. Prognostic value of multidetector computed tomography coronary angiography in diabetes: excellent long-term prognosis in patients with normal coronary arteries. Diabetes Care 2013;36:1834–41.

[29] Feuchtner G, Goetti R, Plass A, et al. Adenosine stress high-pitch 128-slice dual-source myocardial computed tomography perfusion for imaging of reversible myocardial ischemia: comparison with magnetic resonance imaging. Circ Cardiovasc Imaging 2011;4:540–9.

[30] Hausleiter J, Martinoff S, Hadamitzky M, et al. Image quality and radiation exposure with a low tube voltage protocol for coronary CT angiography results of the PROTECTION II trial. JACC Cardiovasc Imaging 2010;3:1113–23.

[31] Ho KT, Ong HY, Tan G, et al. Dynamic CT myocardial perfusion measurements of resting and hyperaemic blood flow in low-risk subjects with 128-slice dual-source CT. Eur Heart J Cardiovasc Imaging 2015;16:300–6.

[32] Linde JJ, Kühl JT, Hove JD, et al. Transmural myocardial perfusion gradients in relation to coronary artery stenoses severity assessed by cardiac multidetector computed tomography. Int J Cardiovasc Imaging 2015;31:171–80.

[33] Byrne C, Kuhl JT, Zacho M, et al. Sex- and age-related differences of myocardial perfusion at rest assessed with multidetector computed tomography. J Cardiovasc Comput Tomogr 2013;7:94–101.